Cellular Autophagy in α Cells Plays a Role in the Maintenance of Islet Architecture

Miwa Himuro,[1] Takeshi Miyatsuka,[1,2] Luka Suzuki,[1,2] Masaki Miura,[1] Takehiro Katahira,[1] Hiromasa Goto,[1] Yuya Nishida,[1] Shugo Sasaki,[3] Masato Koike,[4] Chiyo Shiota,[5] George K. Gittes,[5] Yoshio Fujitani,[6] and Hirotaka Watada[1,2,7]

[1]Department of Metabolism and Endocrinology, Juntendo University Graduate School of Medicine, Tokyo 113-8421, Japan; [2]Center for Identification of Diabetic Therapeutic Targets, Juntendo University Graduate School of Medicine, Tokyo 113-8421, Japan; [3]Department of Surgery, The University of British Columbia, Vancouver BC V5Z4H4, Canada; [4]Departments of Cell Biology and Neurosciences, Juntendo University Graduate School of Medicine, Tokyo 113-8421, Japan; [5]Division of Pediatric Surgery, Department of Surgery, Children's Hospital of Pittsburgh of UPMC, University of Pittsburgh School of Medicine, Pittsburgh, Pennsylvania 15224; [6]Laboratory of Developmental Biology & Metabolism, Institute for Molecular & Cellular Regulation, Gunma University, Maebashi 371-8512, Japan; and [7]Center for Therapeutic Innovations in Diabetes, Juntendo University Graduate School of Medicine, Tokyo 113-8421, Japan

ORCiD numbers: 0000-0003-2618-3450 (T. Miyatsuka).

Autophagy is known to play a pivotal role in intracellular quality control through the degradation of subcellular damaged organelles and components. Whereas autophagy is essential for maintaining β-cell function in pancreatic islets, it remains unclear as to how the cellular autophagy affects the homeostasis and function of glucagon-secreting α cells. To investigate the role of autophagy in α cells, we generated a mutant mouse model lacking *Atg7*, a key molecule for autophagosome formation, specifically in α cells. Histological analysis demonstrated more glucagon-positive cells, with a multilayered structure, in the islets under *Atg7* deficiency, although metabolic profiles, such as body weight, blood glucose, and plasma glucagon levels were comparable between *Atg7*-deficient mice and control littermates. Consistent with our previous findings that *Atg7* deficiency suppressed β-cell proliferation, cellular proliferation was suppressed in *Atg7*-deficient α cells. These findings suggest that α-cell autophagy plays a role in maintaining α-cell area and normal islet architecture but appears to be dispensable for metabolic homeostasis.

Freeform/Key Words: autophagy, Atg7, α cell, islet

Autophagy is an evolutionarily conserved process involving the degradation of cellular components and is known to be stimulated during starvation, cellular and tissue remodeling, and cell death [1]. Furthermore, autophagy plays an essential role in the proper functioning of various kinds of cells, including insulin-producing pancreatic β cells [2]. Several studies have demonstrated that increased numbers of autophagosomes are observed in β cells of patients with diabetes and mice with diabetes [3–6]. Moreover, β-cell–specific knockout of *Atg7*, which is an essential gene for autophagy, resulted in impaired glucose tolerance, accompanied by insufficient insulin secretion and reduced β-cell mass [4, 7]. Thus, accumulating evidence has highlighted the role of autophagy in maintaining β-cell homeostasis in pancreatic islets,

Abbreviations: DAPI, 4,6-diamidino-2-phenylindole; ITT, insulin tolerance test; TFEB, transcription factor EB.

Received 22 February 2019
Accepted 22 July 2019
First Published Online 8 August 2019

ISSN 2472-1972
November 2019 | Vol. 3, Iss. 11
doi: 10.1210/js.2019-00075 | Journal of the Endocrine Society | 1979–1992

whereas it remains unclear as to how cellular autophagy affects the homeostasis and function of glucagon-secreting α cells, which are another type of pancreatic endocrine cell.

Pancreatic α cells play an essential role in elevating plasma glucose levels through glucagon secretion [8]. In addition, it has been known for decades that not only insufficient insulin secretion from β cells but also inappropriate glucagon secretion from α cells is involved in the pathophysiology of diabetes [9–11]. Therefore, a better understanding of α-cell biology will lead to an integral comprehension of glucose homeostasis and the development of diabetes.

In the current study, we hence investigated the role of autophagy in α cells using a mutant mouse model lacking *Atg7*, which is a key molecule of autophagosome formation, and found that α-cell autophagy is required for maintaining normal α-cell architecture and cellular proliferation, whereas it is dispensable for metabolic homeostasis.

1. Methods

A. Animals

GFP-LC3 transgenic mice, floxed *Atg7* ($Atg7^{flox/flox}$) mice, and $Gcg^{CreERT2/+}$ knock-in mice were generated as described previously [12–14]. Mouse genotypes were determined by PCR using DNA from tail biopsies. Tamoxifen (Sigma-Aldrich, St. Louis, MO) was prepared at 20 mg/mL in corn oil. For induction of Cre-mediated recombination, the mice were subcutaneously injected with 4 mg of tamoxifen at the age of 4 weeks, three times over a 1-week period. For the induction of autophagy, an inhibitor of mammalian target of rapamycin, Torin 1 (TOCRIS, Bristol, UK) was administered to C57BL/6J mice at the age of 8 weeks, as previously described [15].

Mice were housed on a 12-hour light-dark cycle in a controlled climate. All studies involving mice were reviewed and approved by the Animal Care and Use Committee of Juntendo University.

B. Measurement of Metabolic Parameters

Glucose tolerance tests were performed after an 8-hour fast by IP injection of glucose (2 g/kg body weight) at the age of 10 weeks. Insulin tolerance tests (ITTs) were performed after a 6-hour fast by the IP injection of insulin (0.75 U/kg body weight) at the age of 8 weeks. Blood glucose levels and plasma glucagon levels were measured using a portable glucose meter (Sanwa Kagaku Co., Ltd., Nagoya, Japan) and glucagon ELISA kit (Mercodia, Uppsala, Sweden, RRID: AB_2783839 [16]), respectively. Plasma amino acid profiles were assayed by liquid chromatography-tandem mass spectrometry.

C. Histology and Immunostaining

Tissues were fixed in 4% paraformaldehyde in PBS at 4°C, washed in PBS, immersed in sucrose solution, and embedded in Tissue-Tek (OCT Compound, Sakura, Tokyo, Japan), or processed routinely for paraffin embedding. Sections were blocked with 1% horse serum, incubated with primary antibodies overnight at 4°C, and then visualized by incubation with secondary antibodies for 30 minutes at room temperature. The primary antibodies used in this study were the following: guinea pig anti-insulin (1:5; Dako, Carpinteria, CA, RRID: AB_2800361 [17]), rat anti-insulin (1:200; R&D Systems, Minneapolis, MN, RRID: AB_2126533 [18]), rabbit antiglucagon (1:1000; Dako, RRID: AB_10013726 [19]), guinea pig antiglucagon (1:1000, Takara Bio, Shiga, Japan, RRID: AB_2619627 [20]), goat anti–transcription factor EB (TFEB; 1:200; Abcam, Cambridge, MA, RRID: AB_303224 [21]), rabbit antichromogranin (1:300; Abcam, RRID: AB_301704 [22]), guinea pig antihuman p62 (1:400, Progen Heidelberg, Germany, RRID: AB_2687531 [23]), mouse anti-Ki67 (1:1000, BD Pharmingen, New Jersey, NJ, RRID: AB_393778 [24]). Cell nuclei were stained with 4,6-diamidino-2-phenylindole (DAPI; Polysciences, Inc., Warrington, PA). For the detection of TFEB and Ki67, mounted sections were microwaved at 95°C for 20 minutes in citrate buffer

(pH 6.0) for antigen retrieval, before being incubated with blocking serum. Terminal deoxynucleotidyl transferase dUTP nick end labeling (TUNEL) staining was performed with *in situ* Apoptosis Detection Kit (Takara Bio, RRID: AB_2800362 [25]). The secondary antibodies used were Alexa Fluor 555-conjugated anti-rabbit IgG (RRID: AB_162543 [26]), Alexa Fluor 555-conjugated anti-mouse IgG (RRID: AB_2536180 [27]), Alexa Fluor 555-conjugated anti-goat IgG (RRID: AB_2535853 [28]), Alexa Fluor 488-conjugated anti-guinea pig IgG (RRID: AB_2534117 [29]), Alexa Fluor 488-conjugated anti-rabbit IgG (RRID: AB_143165 [30]), Alexa Fluor 488-conjugated anti-rat IgG (RRID: AB_2535794 [31]), (all at 1:200; Invitrogen, Carlsbad, CA). After washing in PBS, sections were mounted in Vectashield mounting medium (Vector Laboratories, Burlingame, CA). Slides were imaged on a Leica TCS SP5 confocal laser scanning microscope (Leica Microsystems, Wetzlar, Germany).

The α-cell area was determined from three different sections separated by at least 100 μm. Images were captured with a Keyence BZ-X700 fluorescence microscope (Keyence, Osaka, Japan) and measured using a BZ-X analyzer (Keyence).

D. Electron Microscopy

Transmission electron microscopic analysis was performed as previously described [4]. Briefly, mice were fixed by cardiac perfusion with 2% glutaraldehyde in 0.1 mL/L phosphate buffer (pH7.4). Samples were embedded in epoxy resin. Semithin sections were cut and stained with toluidine blue. Ultrathin sections (80-nm thick) were cut and observed with a Hitachi HT7700 electron microscope (Hitachi, Tokyo, Japan). Cell types within islets were distinguished by the specific appearance of secretory granules [32].

E. Statistical Analyses

Statistical analyses were performed using SPSS 18.0 for Windows (SPSS Inc., Chicago, IL). Comparisons of two samples were performed by unpaired two-tailed *t*-tests. Multiple groups were analyzed by one-way ANOVA with a multiple comparison test. $P < 0.05$ was considered to indicate a statistically significant difference between two groups. Data are presented as the mean ± SE.

2. Results

A. Comparison of Autophagy Status in α Cells Between Fed and Fasted Conditions

To investigate autophagic status in pancreatic α cells, we used *GFP-LC3* reporter mice, in which autophagosome formation can be visualized as green fluorescent puncta [12] and performed immunostaining for glucagon to label α cells (Fig. 1A). Quantification of green fluorescent puncta in α cells demonstrated an increase in the number of puncta after a 30-hour fast compared with under fed conditions (Fig. 1B). Furthermore, TFEB, an essential inducer for autophagy [33], was clearly observed in the nuclei of α cells after the 30-hour fast (Fig. 2A), which is similar to the control experiment using an inhibitor of mammalian target of rapamycin, Torin 1 (Fig. 2B). In addition, data analysis based on single-cell RNA sequencing of the human pancreas, which was reported by Segerstolpe *et al.* [34], demonstrated that *TFEB* mRNA was highly expressed in human α cells as well as in β cells (Fig. 2C). These findings suggest that pancreatic α cells exhibit two distinct phases of autophagy status between fed and fasted conditions, as seen in most other cell types such as acinar cells and hepatocytes [12].

B. Generation of α-Cell–Specific Atg7-Deficient Mice

To investigate the role of cellular autophagy in α cells, floxed *Atg7* ($Atg7^{flox/flox}$) mice were crossed with $Gcg^{CreERT2/+}$ mice [14], which express tamoxifen-inducible Cre recombinase under the control of the proglucagon promoter, to delete *Atg7* in α cells, but not in other endocrine cells in the islets of double-mutant mice ($Gcg^{CreERT2/+}$; $Atg7^{flox/flox}$ ($\alpha Atg7KO$)). When Cre-mediated *Atg7* deletion was induced by subcutaneous injection of tamoxifen at the

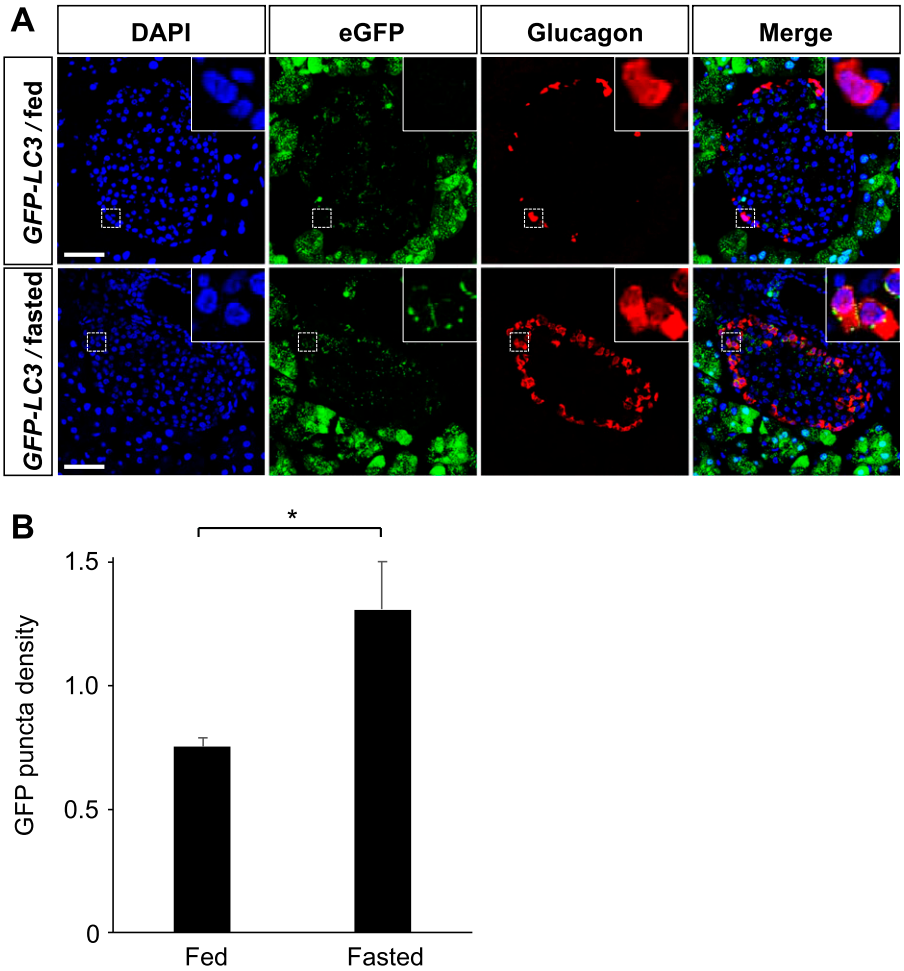

Figure 1. Autophagy status in α cells. (A) Immunostaining for glucagon (red) was performed in *GFP-LC3* transgenic mice at the age of 12 wk under fed (upper panels) and fasted (middle and bottom panels) conditions. Nuclei were labeled with DAPI (blue). Whereas few green-fluorescent LC3 puncta were detected in α cells under the fed condition, a large number of green fluorescent puncta were observed after 30-h fasting. Scale bars, 50 μm. (B) The number of green fluorescent puncta in α cells was quantified in *GFP-LC3* mice (males and females) under fed and 30-h–fasted conditions (n = 3 mice in each group). Data are presented as the mean ± SE. $^*P < 0.05$. eGFP, enhanced green fluorescent protein.

age of 4 weeks (Fig. 3A), the accumulation of p62, which is an adaptor protein for autophagy, was observed in more than 90% of α cells of 10-week-old *αAtg7KO* mice, and the number and size of p62 puncta were increased with age (Fig. 3B), whereas there was no detectable staining of p62 in control littermates. Because p62 has been shown to be degraded by autophagy [35], the specific and substantial accumulation of p62 in α cells, but not in other endocrine cells in the islets, indicates that autophagic failure is efficiently induced in a tamoxifen-inducible manner in *αAtg7KO* mice, as we originally designed. In addition to immunofluorescence imaging, electron microscopic analysis of *αAtg7KO* mice confirmed the induction of autophagic failure in α cells, demonstrated by the presence of inclusion bodies, deformed mitochondria, and concentric membranous structures, which were consistent with the findings in other cell types under *Atg7* deficiency (Fig. 3C–3F) [13].

C. Comparable Metabolic Profiles Between αAtg7KO and Control Mice

To investigate whether *Atg7* deficiency in α cells affects metabolic homeostasis, we investigated various metabolic parameters, such as body weight, glucose tolerance, insulin

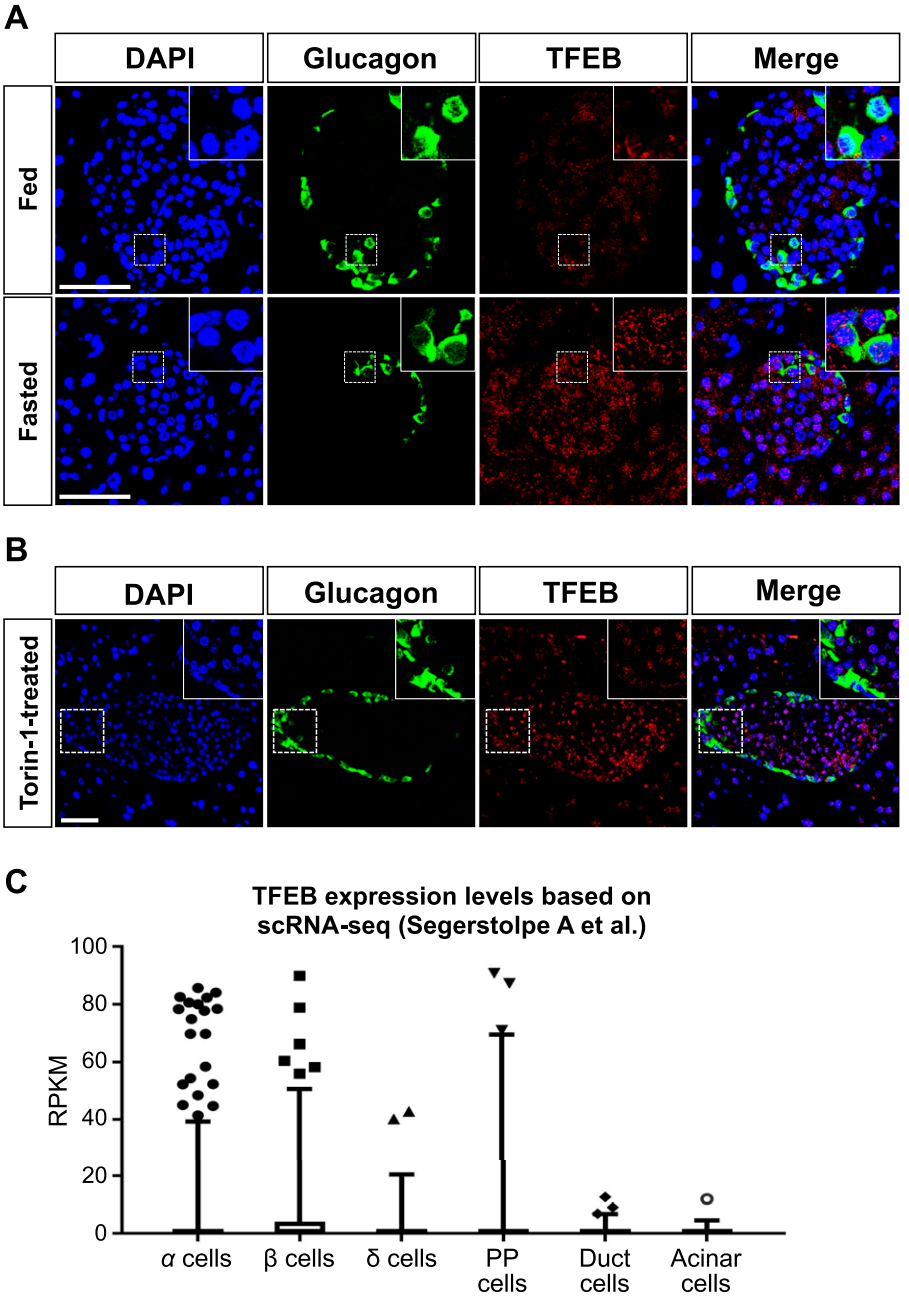

Figure 2. TFEB expression in α cells. (A) Immunostaining for glucagon (green) and TFEB (red) was performed in C57BL/6J male mice at the age of 8 wk under fed (upper panels) and fasted (bottom panels) conditions. Nuclei were labeled with DAPI (blue). Scale bars, 50 μm. (B) Torin 1 was injected to 8-wk-old *C57BL/6J* mice that were euthanized 2 h later. Immunostaining for glucagon (green) and TFEB (red) was performed in the pancreas. Nuclei were labeled with DAPI (blue). (C) Boxplot of *TFEB* expression levels based on single-cell RNA sequencing data of five healthy human subjects, as published by Segerstolpe *et al.* [34]. The original transcriptome data were downloaded through EMBL-EBI (accession number: E-MTAB-5060 and 5061). The boxes mark the interval between the 25th and 75th percentiles. The whiskers denote the interval between the 5th and 95th percentiles. Markers above whiskers indicate data points outside the 5th and 95th percentiles. Data are presented as the mean ± SE. RPKM, reads per kilobase of transcript per million mapped reads.

tolerance, and plasma glucagon levels. When *Atg7* deficiency was induced at 4 weeks of age, body weights and random blood glucose levels were comparable between *αAtg7KO* and control littermates until the age of 10 weeks (Fig. 4A and 4B). Blood glucose levels during the

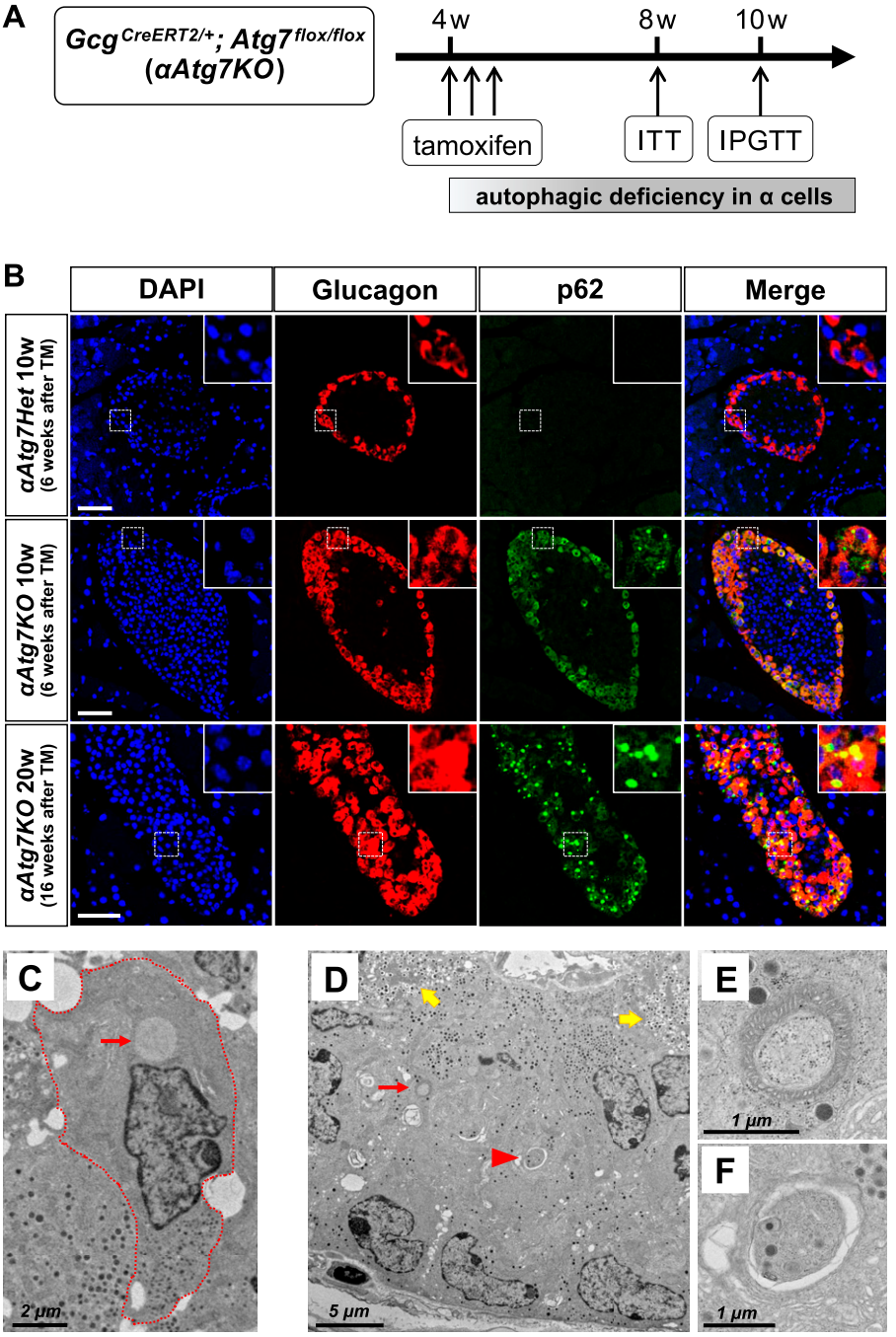

Figure 3. Generation of α-cell–specific *Atg7*-deficient mice and their histological abnormalities. (A) Diagram showing the induction method of Cre-mediated inactivation of *Atg7* specifically in α cells. ITTs and IP GTTs were performed at the age of 8 and 10 wk, respectively. (B) Immunostaining for p62 (green) and glucagon (red) was performed in *αAtg7KO* mice (males and females) and control littermates at the age of 10 and 20 wk. Tamoxifen was injected into both $Gcg^{CreERT2/+}$; $Atg7^{flox/flox}$ (*αAtg7KO*) mice and $Gcg^{CreERT2/+}$; $Atg7^{flox/+}$ (*αAtg7Het*) mice at the age of 4 wk. Nuclei were labeled with DAPI (blue). Accumulation of p62 was observed specifically in α cells of *αAtg7KO* mice but not in *αAtg7Het* mice. Scale bars, 50 μm. (C–F) Electron microscopic analysis demonstrating the presence of inclusion body [arrow in (C); dotted line in (C) outlines the cell boundary], deformed mitochondria [red arrow in (D) and enlarged in (E)], and concentric membranous structures [red arrowhead in (D) and enlarged in (F)] were observed in α cells of 10-wk-old *αAtg7KO* male mice. β cells are indicated with yellow arrows in (D).

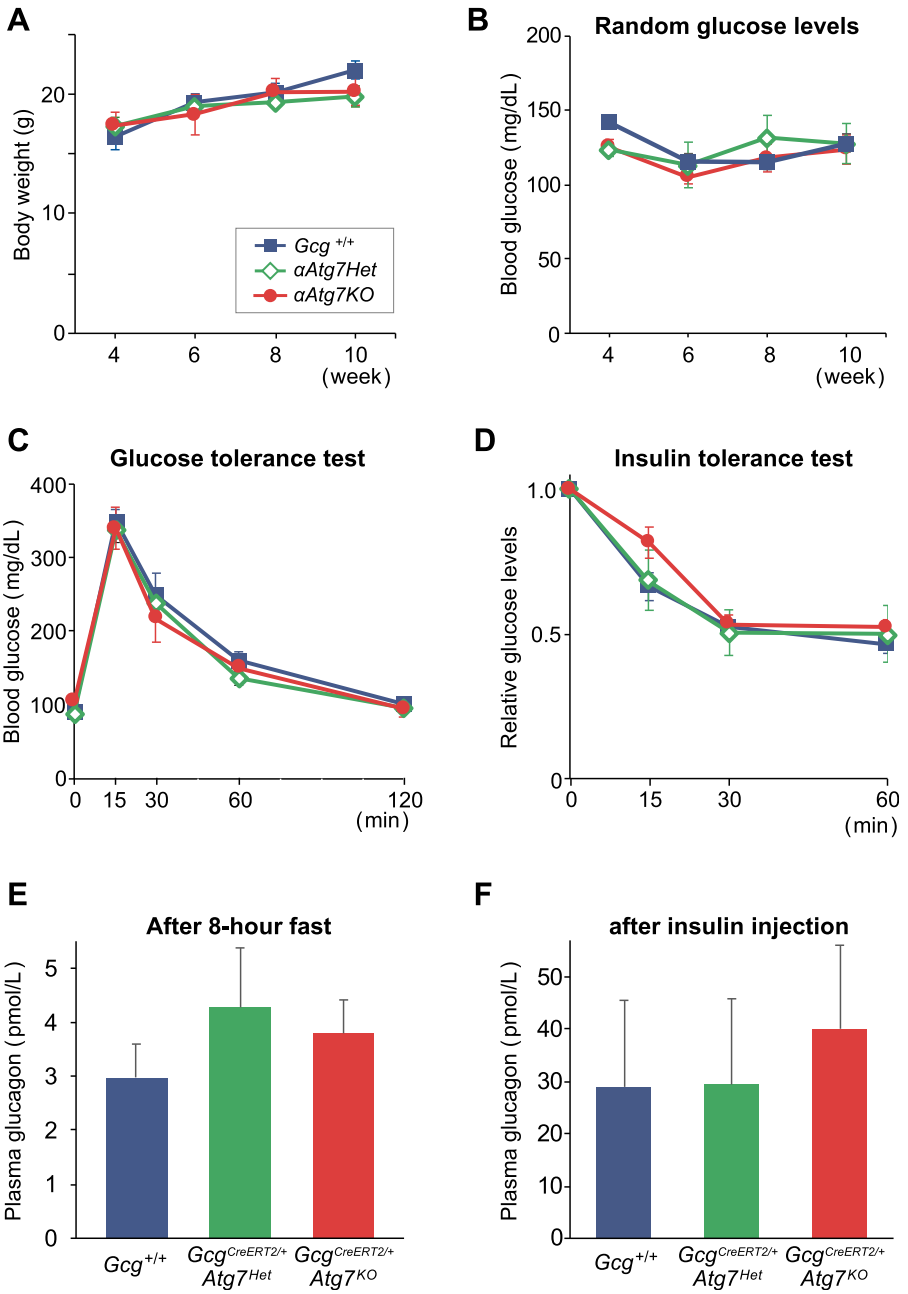

Figure 4. Metabolic profiles are comparable between *αAtg7KO* and the control mice. (A) Body weights and (B) random blood glucose levels of $Gcg^{+/+}$, $Gcg^{CreERT2/+}$; $Atg7^{flox/+}$ (*αAtg7Het*), and *αAtg7KO* male mice were measured every 2 wk (n = 6 to 11 mice for each group) until the age of 10 wk. (C) Blood glucose levels were measured during the IP GTT at the age of 10 wk, 6 wk after tamoxifen injection, as indicated in Figure 3A. (D) ITTs were performed at the age of 8 wk, 4 wk after the tamoxifen injection. (E) Plasma glucagon levels were measured after an 8-h fast at the age of 10 wk. (F) Plasma glucagon levels were measured 30 min after IP insulin injection at the age of 10 weeks. In (C–F), n = 3 to 5 mice for each group. Data are presented as the mean ± SE.

glucose tolerance test (GTT) and ITT showed no difference between the groups (Fig. 4C and 4D). In addition, plasma glucagon levels, which were measured after an 8-hour fast or after insulin injection during the ITT, were not different between *αAtg7KO* and control littermates at the age of 10 weeks (Fig. 4E and 4F). Furthermore, whereas suppressed glucagon signaling is reported to affect the profiles of circulating amino acids [36, 37], there were no changes in

plasma amino acid composition between the groups (Table 1). Taken together, we did not find any effects of the autophagic failure in α cells on metabolic homeostasis, at least regarding the parameters that we assessed under our experimental conditions.

D. Abnormal Distribution of α Cells in the Islets of αAtg7KO Mice

Immunostaining for glucagon, insulin, and chromogranin A demonstrated that there was no difference in total endocrine cell area, total α-cell area, and total non-α–cell area across the pancreas between the groups (Fig. 5). On the other hand, more detailed observation of individual islets revealed that some islets of *αAtg7KO* mice had a large number of α cells, with multiple-layered structures (Fig. 6A), and other islets appeared normal with α cells peripherally located around insulin-producing β cells. To evaluate the changes in α-cell distribution in *αAtg7KO* mice statistically, scatter plots between α-cell area and total endocrine area were made using α-cell ratios in the islets calculated by immunostaining for glucagon and chromogranin A (Fig. 6B and 6C), which demonstrated that the percentage of the islets with higher α-cell ratios (>0.25) was higher in *αAtg7KO* mice than in control littermates (Fig. 6D).

To investigate whether a higher α-cell ratio in *αAtg7KO* mice was a result of increased α-cell proliferation, immunostaining for glucagon and Ki67 was performed. Contrary to our expectation, the number of Ki67-positive cells was decreased in *αAtg7KO* mice (Fig. 7A and 7B), which suggests that autophagy deficiency suppresses α-cell proliferation. On the other hand, TUNEL staining showed that α-cell apoptosis was not decreased in *αAtg7KO* mice (Fig. 7C). Thus, the higher α-cell ratios of *αAtg7KO* mice do not appear to be a result of increased α-cell proliferation or decreased apoptosis.

3. Discussion

Although several studies have demonstrated that autophagy plays a role in cellular homeostasis in pancreatic β cells [4, 7, 38, 39], it remains to be elucidated as to how α-cell function is regulated by autophagy. In this study, we investigated the role of cellular autophagy in α-cell homeostasis in mice.

Table 1. Amino Acids in Serum from *αAtg7KO* Mice and Control Littermates

		Control			*αAtg7KO*			
Amino Acid		**Mean**	**±**	**SE**	**Mean**	**±**	**SE**	***P***
Alanine	Ala	262.1	±	34.3	242.2	±	39.3	0.722
Cystine	Cys	16.4	±	5.2	17.7	±	8.6	0.903
Aspartic acid	Asp	6.9	±	1.9	4.6	±	1.0	0.341
Glutamic acid	Glu	21.6	±	5.2	16.8	±	1.3	0.424
Phenylalanine	Phe	75.2	±	7.6	64.8	±	3.9	0.291
Glycine	Gly	317.3	±	44.4	296.9	±	24.1	0.708
Histidine	His	59.3	±	9.3	51.1	±	6.4	0.508
Isoleucine	Ile	82.0	±	15.8	83.5	±	16.2	0.951
Lysine	Lys	226.8	±	47.5	215.4	±	26.1	0.844
Leucine	Leu	116.0	±	26.9	118.3	±	25.3	0.955
Methionine	Met	56.4	±	10.3	43.4	±	7.0	0.355
Asparagine	Asn	35.7	±	8.6	32.5	±	2.7	0.738
Proline	Pro	85.1	±	15.7	65.8	±	7.7	0.332
Glutamine	Gln	601.5	±	58.6	635.9	±	120.8	0.810
Arginine	Arg	72.2	±	0.5	73.8	±	13.4	0.909
Serine	Ser	95.3	±	9.8	90.3	±	7.9	0.713
Threonine	Thr	99.2	±	7.5	92.1	±	4.3	0.457
Valine	Val	157.4	±	9.3	150.4	±	8.4	0.606
Tryptophan	Trp	54.7	±	11.8	51.6	±	5.5	0.828
Tyrosine	Tyr	70.5	±	33.2	52.7	±	8.4	0.630

Plasma amino acids profiles were assayed in *αAtg7KO* mice and control littermates at 10 wk of age (n = 3; males and females in each group), which was 6 wk after the first tamoxifen injection. Data are presented as mean ± SE.

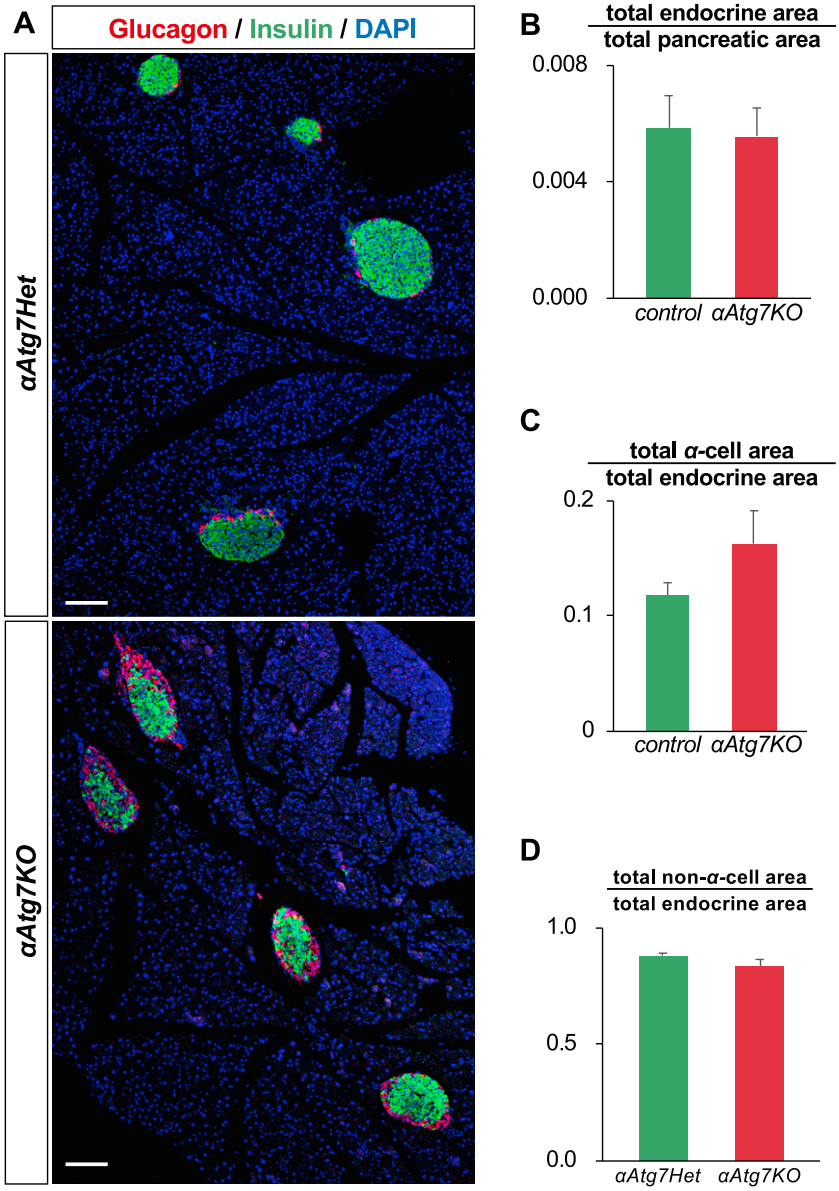

Figure 5. Distribution of α and β cells in the islets of *αAtg7KO* mice. (A) Immunostaining for insulin (green) and glucagon (red) was performed in the pancreata of *αAtg7KO* male mice and control littermates. Scale bars, 100 μm. (B–D) Total pancreatic areas and α-cell areas were measured based on immunostaining for glucagon. The ratio of (B) total endocrine area to total pancreatic area, (C) total α-cell area to total endocrine cell area, and (D) total non–α-cell area to total endocrine cell area were displayed as bar graphs. In (B–D), n = 3 mice for each group. Data are presented as the mean ± SE.

Our results demonstrated several similarities and differences in the regulation and roles of autophagy between α and β cells. First, immunofluorescence imaging of *GFP-LC3* puncta revealed that the number of green-fluorescent puncta in α cells was increased during starvation, like most other cells types [12], whereas green fluorescent puncta in β cells were more easily detected underfed conditions (Fig. 1), which is consistent with a previous study [40]. On the other hand, the nuclear translocation of TFEB was more clearly observed in both α and β cells after a 30-hour fast compared with fed conditions (Fig. 2A), which is in contrast to the findings of *GFP-LC3* puncta described above. Second, *Atg7* deficiency in α cells did not affect metabolic profiles at least regarding the parameters that we tested, whereas

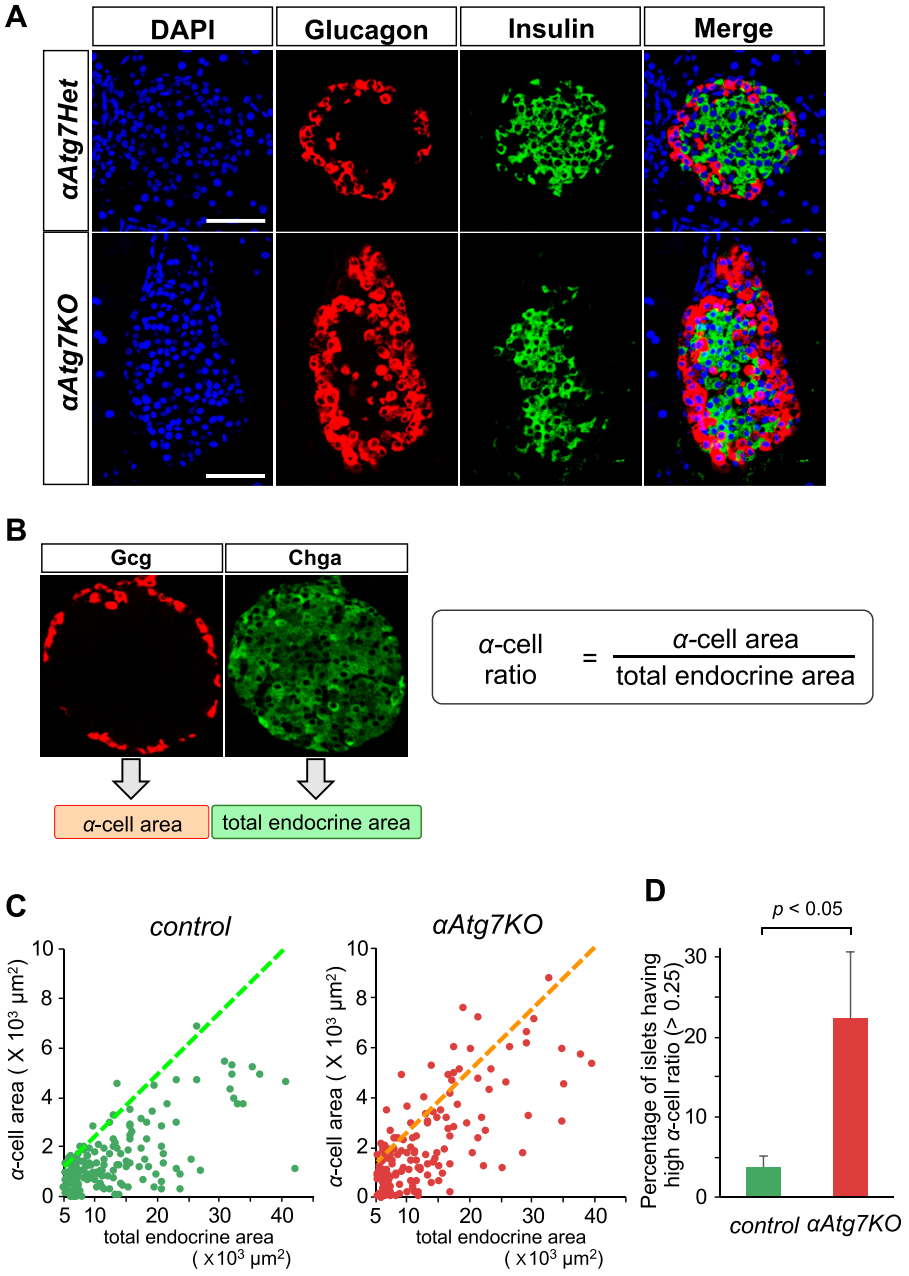

Figure 6. Abnormal distribution of α cells in the islets of *αAtg7KO* mice. (A) Immunostaining for insulin (green) and glucagon (red) was performed in the pancreas of *αAtg7KO* male mice and the control male littermates. Nuclei were labeled with DAPI (blue). Multilayered α cells were observed in the islets of *αAtg7KO* mice. Scale bars, 50 μm. (B) A schematic diagram of the experimental strategy used to calculate the α-cell ratio for each islet from *αAtg7KO* mice. Immunostaining for glucagon (red) and chromogranin A (green) was performed and then α-cell ratio was calculated as shown on the right. (C) Scatter plots representing α-cell area vs total endocrine area in the pancreata of control littermates (green plots, n = 4 mice) and *αAtg7KO* mice (red plot, n = 3 mice). Each dot stands for one islet that was used for measuring α-cell area per cell and endocrine-cell area per cell. Control littermates include $Gcg^{CreERT2/+}$; $Atg7^{flox/+}$ (*αAtg7Het*) and $Gcg^{CreERT2/+}$; $Atg7^{+/+}$. (D) A bar graph showing the percentage of islets in which the α-cell ratio was more than 0.25 (dotted lines in the scatter plots). Chga, chromogranin A; Gcg, glucagon.

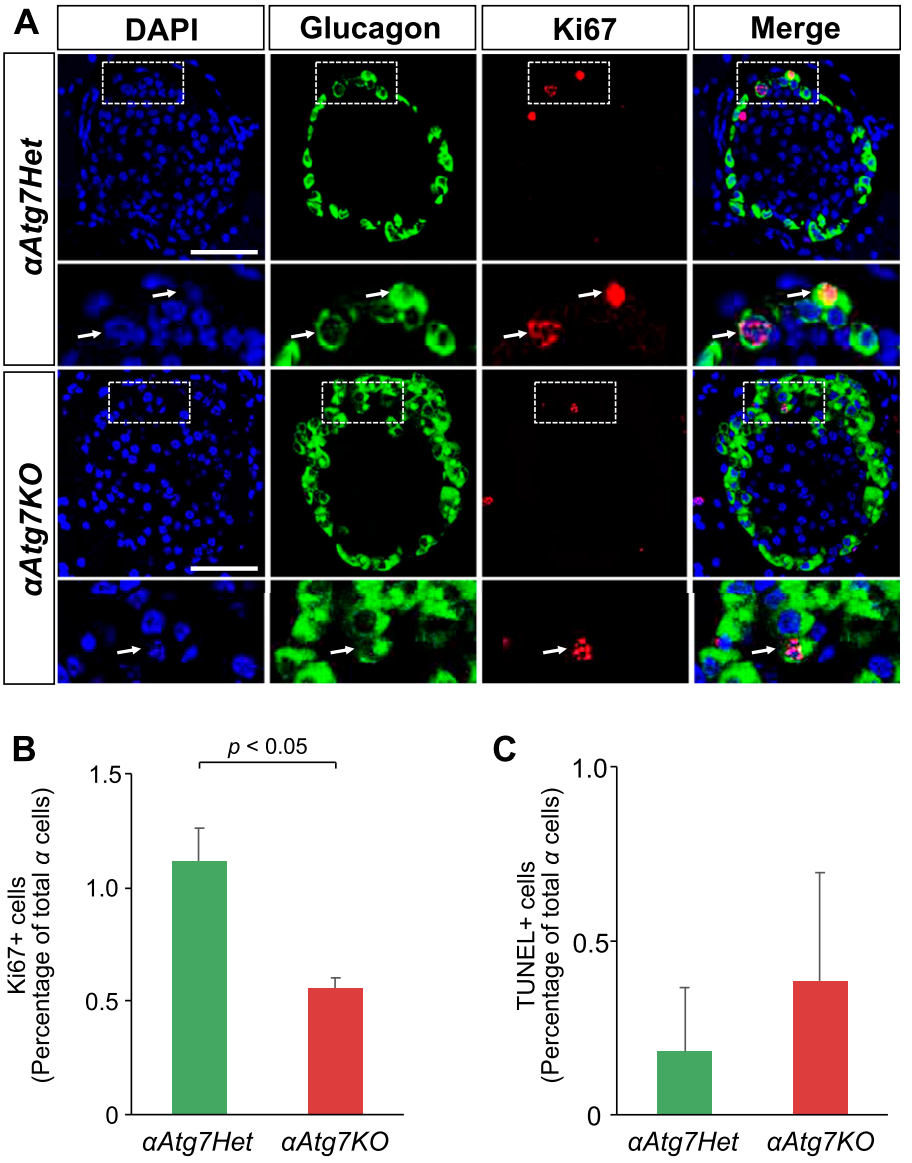

Figure 7. Cellular proliferation and viability in islets of *αAtg7KO* mice. (A) Immunostaining for glucagon (green) and Ki67 (red) was performed in the pancreas of *αAtg7KO* mice and control littermates. Nuclei were labeled with DAPI (blue). Colocalization of Ki67 and glucagon is indicated by arrows. Scale bars, 50 μm. (B) The percentage of Ki67-positive cells in total α cells was displayed in the bar graph (right panel, n = 4 mice, more than 20 islets from each mouse). (C) The percentage of TUNEL-positive cells among total α cells shown as a bar graph (n = 3 mice, more than 10 islets from each mouse). Control littermates include $Gcg^{CreERT2/+}$; $Atg7^{flox/+}$ and $Gcg^{CreERT2/+}$; $Atg7^{+/+}$. All mice used in these experiments were euthanized at 10 wk of age, 6 wk after the first tamoxifen injection. Data are presented as the mean ± SE.

β-cell–specific *Atg7* deficiency (*βAtg7KO*) resulted in impaired glucose tolerance. Last, α-cell ratios were increased in *αAtg7KO* mice, whereas *βAtg7KO* mice had decreased β-cell mass under a high-fat diet [4], although both *αAtg7KO* and *βAtg7KO* mice showed suppressed cellular proliferation. The opposite roles of these two types of endocrine cells in regulating glucose homeostasis between reflect such distinct phenotypes.

Disarranged and/or multiple-layered α cells were detected in several islets of *αAtg7KO* mice, where α-cell area was increased (Fig. 6A, 6C, and 6D), although many other islets had

relatively normal α-cell area. These findings suggest that autophagy is essential for maintaining proper α-cell architecture in the islets. Increased α-cell mass had been reported in several mouse models, in which glucagon itself or glucagon receptor signaling was suppressed [41–43]. In these mouse models, hepatic gene expression is altered, which results in high levels of serum amino acids such as glutamine [19, 20]. Whereas these mouse models demonstrated increased α-cell proliferation, the number of proliferating α cells in *αAtg7KO* mice was decreased compared with control littermates (Fig. 6B). In addition, plasma profiles of glucagon and amino acids were comparable between the groups (Fig. 4E; Table 1). These findings suggest that the underlying molecular mechanisms by which α-cell ratio was increased in *αAtg7KO* mice are totally different from those in the other mouse models described above. Higher α-cell ratios without increased α-cell proliferation or decreased apoptosis (Fig. 7) suggest the possibility that α-cell neogenesis from the non–α-cell population causes such α-cell architecture under *Atg7* deficiency.

Immunohistological observation of the pancreas revealed that not all the islets had a high α-cell ratio, that is, there was heterogeneity in α-cell area among the islets of *αAtg7KO* mice (Fig. 6B). The accumulation of p62 puncta was observed in most α cells throughout the islets (Fig. 3B), showing that the autophagic failure was homogeneously induced in α cells as we originally designed. Therefore, it would be difficult to explain the heterogeneity of α-cell architecture solely by incomplete Cre-mediated recombination. To address this question, the circumstances in which abnormal islets with high α-cell ratio are formed need to be clarified.

Disruption of α-cell homeostasis as well as β-cell failure have been shown to lead to impaired glucose tolerance [9–11], and the general importance of autophagy for cell homeostasis as well as its involvement in human diseases [44] tempted us to investigate the role of α-cell autophagy in glucose metabolism. Our present study demonstrated that the effects of autophagic dysfunction in α cells are substantially different from the effects in β cells, showing that *Atg7* deficiency in α cells did not elicit substantial changes in metabolic profiles. There is still the possibility that *Atg7* deficiency in α cells may affect metabolic profiles under certain circumstances. For example, aged *Atg7*-deficient mice may have distinct phenotypes from younger mice. In addition, measuring glucagon and GLP-1 secretion *ex vivo* in isolated islets would be important for clarifying the differences between *αAtg7KO* and control mice. Thus, further studies are essential for uncovering the role of autophagy in α cells.

Acknowledgments

We thank Hiroko Tsujimura, Sumie Ishikawa, and Yasuko Hirakawa for their excellent technical assistance. We also acknowledge the support of the mouse facility and the cell imaging core, Division of Molecular and Biochemical Research, and Research Support Center at Juntendo University.

Financial Support: This work was supported by research grants from Daiichi-Sankyo, Inc., Takeda Pharmaceutical Company Ltd., Kyowa Hakko Kirin Company, Ltd. (to T.M. and H.W.), JSPS KAKENHI (no. 16K15490, 17K09848, and 17H04202), and Japan Agency for Medical Research and Development [JP18gm0610005 (to Y.F.)].

Additional Information

Correspondence: Takeshi Miyatsuka, MD, PhD, Juntendo University Graduate School of Medicine, 2-1-1 Hongo, Bunkyo-ku, Tokyo 113-8421, Japan. E-mail: miyatsuka-takeshi@umin.net.

Disclosure summary: The authors have nothing to disclose.

Data Availability: All data generated or analyzed during this study are included in this published article or in the data repositories listed in References.

References and Notes

1. Levine B, Klionsky DJ. Development by self-digestion: molecular mechanisms and biological functions of autophagy. *Dev Cell.* 2004;**6**(4):463–477.
2. Watada H, Fujitani Y. Minireview: autophagy in pancreatic β-cells and its implication in diabetes. *Mol Endocrinol.* 2015;**29**(3):338–348.

3. Masini M, Bugliani M, Lupi R, del Guerra S, Boggi U, Filipponi F, Marselli L, Masiello P, Marchetti P. Autophagy in human type 2 diabetes pancreatic beta cells. *Diabetologia*. 2009;**52**(6):1083–1086.
4. Ebato C, Uchida T, Arakawa M, Komatsu M, Ueno T, Komiya K, Azuma K, Hirose T, Tanaka K, Kominami E, Kawamori R, Fujitani Y, Watada H. Autophagy is important in islet homeostasis and compensatory increase of beta cell mass in response to high-fat diet. *Cell Metab*. 2008;**8**(4):325–332.
5. Quan W, Hur KY, Lim Y, Oh SH, Lee JC, Kim KH, Kim GH, Kim SW, Kim HL, Lee MK, Kim KW, Kim J, Komatsu M, Lee MS. Autophagy deficiency in beta cells leads to compromised unfolded protein response and progression from obesity to diabetes in mice. *Diabetologia*. 2012;**55**(2):392–403.
6. Bachar-Wikstrom E, Wikstrom JD, Ariav Y, Tirosh B, Kaiser N, Cerasi E, Leibowitz G. Stimulation of autophagy improves endoplasmic reticulum stress-induced diabetes. *Diabetes*. 2013;**62**(4):1227–1237.
7. Jung HS, Chung KW, Won Kim J, Kim J, Komatsu M, Tanaka K, Nguyen YH, Kang TM, Yoon KH, Kim JW, Jeong YT, Han MS, Lee MK, Kim KW, Shin J, Lee MS. Loss of autophagy diminishes pancreatic beta cell mass and function with resultant hyperglycemia. *Cell Metab*. 2008;**8**(4):318–324.
8. Gromada J, Franklin I, Wollheim CB. Alpha-cells of the endocrine pancreas: 35 years of research but the enigma remains. *Endocr Rev*. 2007;**28**(1):84–116.
9. Raskin P, Unger RH. Hyperglucagonemia and its suppression. Importance in the metabolic control of diabetes. *N Engl J Med*. 1978;**299**(9):433–436.
10. D'Alessio D. The role of dysregulated glucagon secretion in type 2 diabetes. *Diabetes Obes Metab*. 2011; **13**(Suppl 1):126–132.
11. Unger RH, Cherrington AD. Glucagonocentric restructuring of diabetes: a pathophysiologic and therapeutic makeover. *J Clin Invest*. 2012;**122**(1):4–12.
12. Mizushima N, Yamamoto A, Matsui M, Yoshimori T, Ohsumi Y. In vivo analysis of autophagy in response to nutrient starvation using transgenic mice expressing a fluorescent autophagosome marker. *Mol Biol Cell*. 2004;**15**(3):1101–1111.
13. Komatsu M, Waguri S, Ueno T, Iwata J, Murata S, Tanida I, Ezaki J, Mizushima N, Ohsumi Y, Uchiyama Y, Kominami E, Tanaka K, Chiba T. Impairment of starvation-induced and constitutive autophagy in Atg7-deficient mice. *J Cell Biol*. 2005;**169**(3):425–434.
14. Shiota C, Prasadan K, Guo P, Fusco J, Xiao X, Gittes GK. Gcg ^{CreERT2} knockin mice as a tool for genetic manipulation in pancreatic alpha cells. *Diabetologia*. 2017;**60**(12):2399–2408.
15. Liu Q, Chang JW, Wang J, Kang SA, Thoreen CC, Markhard A, Hur W, Zhang J, Sim T, Sabatini DM, Gray NS. Discovery of 1-(4-(4-propionylpiperazin-1-yl)-3-(trifluoromethyl)phenyl)-9-(quinolin-3-yl) benz o[h][1,6]naphthyridin-2(1H)-one as a highly potent, selective mammalian target of rapamycin (mTOR) inhibitor for the treatment of cancer. *J Med Chem*. 2010;**53**(19):7146–7155.
16. RRID:AB_2783839, http://scicrunch.org/resolver/AB_2783839.
17. RRID:AB_2800361, http://scicrunch.org/resolver/AB_2800361.
18. RRID:AB_2126533, http://scicrunch.org/resolver/AB_2126533.
19. RRID:AB_10013726, http://scicrunch.org/resolver/AB_10013726.
20. RRID:AB_2619627, http://scicrunch.org/resolver/AB_2619627.
21. RRID:AB_303224, http://scicrunch.org/resolver/AB_303224.
22. RRID:AB_301704, http://scicrunch.org/resolver/AB_301704.
23. RRID:AB_2687531, http://scicrunch.org/resolver/AB_268753.
24. RRID:AB_393778, http://scicrunch.org/resolver/AB_393778.
25. RRID:AB_2800362, http://scicrunch.org/resolver/AB_2800362.
26. RRID:AB_162543, http://scicrunch.org/resolver/AB_162543.
27. RRID:AB_2536180, http://scicrunch.org/resolver/AB_2536180.
28. RRID:AB_2535853, http://scicrunch.org/resolver/AB_2535853.
29. RRID:AB_2534117, http://scicrunch.org/resolver/AB_2534117.
30. RRID:AB_143165, http://scicrunch.org/resolver/AB_143165.
31. RRID:AB_2535794, http://scicrunch.org/resolver/AB_2535794.
32. Brereton MF, Vergari E, Zhang Q, Clark A. Alpha-, delta- and PP-cells: are they the architectural cornerstones of islet structure and co-ordination? *J Histochem Cytochem*. 2015;**63**(8):575–591.
33. Settembre C, Di Malta C, Polito VA, Garcia Arencibia M, Vetrini F, Erdin S, Erdin SU, Huynh T, Medina D, Colella P, Sardiello M, Rubinsztein DC, Ballabio A. TFEB links autophagy to lysosomal biogenesis. *Science*. 2011;**332**(6036):1429–1433.
34. Segerstolpe Å, Palasantza A, Eliasson P, Andersson EM, Andréasson AC, Sun X, Picelli S, Sabirsh A, Clausen M, Bjursell MK, Smith DM, Kasper M, Ämmälä C, Sandberg R. Single-cell transcriptome profiling of human pancreatic islets in health and type 2 diabetes. *Cell Metab*. 2016;**24**(4):593–607.
35. Komatsu M, Waguri S, Koike M, Sou YS, Ueno T, Hara T, Mizushima N, Iwata J, Ezaki J, Murata S, Hamazaki J, Nishito Y, Iemura S, Natsume T, Yanagawa T, Uwayama J, Warabi E, Yoshida H, Ishii T,

Kobayashi A, Yamamoto M, Yue Z, Uchiyama Y, Kominami E, Tanaka K. Homeostatic levels of p62 control cytoplasmic inclusion body formation in autophagy-deficient mice. *Cell*. 2007;**131**(6): 1149–1163.

36. Solloway MJ, Madjidi A, Gu C, Eastham-Anderson J, Clarke HJ, Kljavin N, Zavala-Solorio J, Kates L, Friedman B, Brauer M, Wang J, Fiehn O, Kolumam G, Stern H, Lowe JB, Peterson AS, Allan BB. Glucagon couples hepatic amino acid catabolism to mTOR-dependent regulation of α-cell mass. *Cell Reports*. 2015;**12**(3):495–510.
37. Dean ED, Li M, Prasad N, Wisniewski SN, Von Deylen A, Spaeth J, Maddison L, Botros A, Sedgeman LR, Bozadjieva N, Ilkayeva O, Coldren A, Poffenberger G, Shostak A, Semich MC, Aamodt KI, Phillips N, Yan H, Bernal-Mizrachi E, Corbin JD, Vickers KC, Levy SE, Dai C, Newgard C, Gu W, Stein R, Chen W, Powers AC. Interrupted glucagon signaling reveals hepatic α cell axis and role for L-glutamine in α-cell proliferation. *Cell Metab*. 2017;**25**(6):1362–1373.e5.
38. Abe H, Uchida T, Hara A, Mizukami H, Komiya K, Koike M, Shigihara N, Toyofuku Y, Ogihara T, Uchiyama Y, Yagihashi S, Fujitani Y, Watada H. Exendin-4 improves β-cell function in autophagy-deficient β-cells. *Endocrinology*. 2013;**154**(12):4512–4524.
39. Shigihara N, Fukunaka A, Hara A, Komiya K, Honda A, Uchida T, Abe H, Toyofuku Y, Tamaki M, Ogihara T, Miyatsuka T, Hiddinga HJ, Sakagashira S, Koike M, Uchiyama Y, Yoshimori T, Eberhardt NL, Fujitani Y, Watada H. Human IAPP-induced pancreatic β cell toxicity and its regulation by autophagy. *J Clin Invest*. 2014;**124**(8):3634–3644.
40. Goginashvili A, Zhang Z, Erbs E, Spiegelhalter C, Kessler P, Mihlan M, Pasquier A, Krupina K, Schieber N, Cinque L, Morvan J, Sumara I, Schwab Y, Settembre C, Ricci R. Insulin granules. Insulin secretory granules control autophagy in pancreatic β cells. *Science*. 2015;**347**(6224):878–882.
41. Gelling RW, Du XQ, Dichmann DS, Romer J, Huang H, Cui L, Obici S, Tang B, Holst JJ, Fledelius C, Johansen PB, Rossetti L, Jelicks LA, Serup P, Nishimura E, Charron MJ. Lower blood glucose, hyperglucagonemia, and pancreatic alpha cell hyperplasia in glucagon receptor knockout mice. *Proc Natl Acad Sci USA*. 2003;**100**(3):1438–1443.
42. Hayashi Y, Yamamoto M, Mizoguchi H, Watanabe C, Ito R, Yamamoto S, Sun XY, Murata Y. Mice deficient for glucagon gene-derived peptides display normoglycemia and hyperplasia of islet alpha-cells but not of intestinal L-cells. *Mol Endocrinol*. 2009;**23**(12):1990–1999.
43. Gu W, Yan H, Winters KA, Komorowski R, Vonderfecht S, Atangan L, Sivits G, Hill D, Yang J, Bi V, Shen Y, Hu S, Boone T, Lindberg RA, Véniant MM. Long-term inhibition of the glucagon receptor with a monoclonal antibody in mice causes sustained improvement in glycemic control, with reversible alpha-cell hyperplasia and hyperglucagonemia. *J Pharmacol Exp Ther*. 2009;**331**(3):871–881.
44. Mizushima N. A brief history of autophagy from cell biology to physiology and disease. *Nat Cell Biol*. 2018;**20**(5):521–527.